crystals

MDPI

Review

Recent Advances in Graphene and Conductive Polymer Composites for Supercapacitor Electrodes: A Review

Xinwei Cai [1], Kangkang Sun [2], Yangshuai Qiu [1] and Xuan Jiao [3,*]

[1] School of Resources and Environmental Engineering, Wuhan University of Technology, Luoshi Road 122, Wuhan 430070, China; cxw19910520@163.com (X.C.); qiuyangshuai@whut.edu.cn (Y.Q.)
[2] School of Chemical Engineering, The University of Queensland, Brisbane 4072, Australia; kangkang.sun@uq.edu.au
[3] School of Materials Science and Engineering, Southeast University, Southeast Road 2nd, Nanjing 211189, China
* Correspondence: x.jiao@seu.edu.cn; Tel.: +86-188-5102-9068

Abstract: Supercapacitors (SCs) have generated a great deal of interest regarding their prospects for application in energy storage due to their advantages such as long life cycles and high-power density. Graphene is an excellent electrode material for SCs due to its high electric conductivity and highly specific surface area. Conductive polymers (CPs) could potentially become the next-generation SC electrodes because of their low cost, facile synthesis methods, and high pseudocapacitance. Graphene/CP composites show conspicuous electrochemical performance when used as electrode materials for SCs. In this article, we present and summarize the synthesis and electrochemical performance of graphene/CP composites for SCs. Additionally, the method for synthesizing electrode materials for better electrochemical performance is discussed.

Keywords: graphene; conductive polymers; supercapacitor; conductive polymers; binary composites; ternary composites; quaternary composites

Citation: Cai, X.; Sun, K.; Qiu, Y.; Jiao, X. Recent Advances in Graphene and Conductive Polymer Composites for Supercapacitor Electrodes: A Review. *Crystals* **2021**, *11*, 947. https://doi.org/10.3390/cryst11080947

Academic Editors: Nguyen Tuan Hung, Ahmad Ridwan Tresna Nugraha, Teng Yang and John Parthenios

Received: 29 June 2021
Accepted: 11 August 2021
Published: 14 August 2021

1. Introduction

Since its discovery in 2004, graphene has attracted extensive interest, and much research has been carried out to study its physical and chemical properties and explore its applications [1–3]. The peculiar optical, mechanical, and electrical properties of graphene make it promising in many fields, such as material science [3], biomedicine [4,5], environmental treatment [6,7], and energy [8,9]. In particular, graphene plays an important role in the fight against COVID-19, and it has recently inspired novel technologies to defeat the pandemic [10,11]. Graphene is considered one of the most promising electrode materials for SCs due to its large specific surface area (SSA), outstanding electrical conductivity, flexibility, and excellent chemical stability [12–14].

Based on their storage mechanism, SCs can be divided into electrochemical double-layer capacitors (EDLCs) [15] and pseudocapacitors [16]. EDLCs keep energy through charge accumulation at the electrode/electrolyte interface [17]. Specifically, reversible electrostatic attraction occurs between the ions from electrolytes and the oppositely charged electrode surfaces during the charging progress [18]. By contrast, ions leave the electrode's surface and move back in the electrolyte during the discharging progress. Since no charge transfer takes place during the process, EDLCs exhibit a fast charge/discharge rate and superior power performance compared to conventional capacitors. The SSA and porosity of the electrode are key factors affecting the capacitance of EDLCs [19]; theoretically, the larger the SSA of the electrode material, the higher the capacitance value of the EDLC. Using carbon as the electrode material is the primary method for manufacturing EDLCs, such as carbon nano-onions [20], activated carbon (AC) [21], and carbon nanotubes (CNTs) [22]. The theoretical SSA of graphene is up to 2630 m^2 g^{-1} [23], making it one of the most promising electrode materials for the manufacture of EDLCs.

The graphene family can be classified into three types: graphene, graphene oxide (GO), and reduced graphene oxide (RGO) [24]. Graphene is a two-dimensional material comprised of sp2-hybridized carbon atoms. GO is synthesized via a proverbial modified Hummers method [25]. The introduction of oxygenated functional groups (carboxyl, hydroxyl, carbonyl, and epoxy) leads to negative charges on the surface of GO [26]. Due to the sp^3 hybridization of carbon atoms, GO is a non-conductive but hydrophilic material [27] that is different from graphene. RGO can be obtained by reducing GO through chemical, thermal, or electrochemical treatment [28]. After the reduction process of GO, RGO still retains limited oxygenated functional groups and defects, and thus possesses high electric conductivity [29].

However, graphite (flake) is a typical layered compound with strong van der Waals interactions, which can be regarded as the-restacking of single-layer graphene. After the process of exfoliation on graphite, graphene sheets still maintain some layered structures, which are able to hinder the diffusion and mass transfer of electrolytes [30,31]. For example, through scanning electron microscope (SEM) images, Stoller et al. [32] found that agglomerate particles approximately 15–25 μm in diameter were formed during reduction, and the surface of the chemically modified graphene (CMG) agglomerate was only 705 $m^2 \cdot g^{-1}$ under the condition that both sides of the individual sheets at the surface of the agglomerate were exposed to the electrolyte. Moreover, in aqueous and organic electrolytes, the specific capacitances of CMG were only 135 and 99 $F \cdot g^{-1}$, respectively.

Therefore, researchers have used various methods, such as chemical activation [33] and physical modification [34], to eliminate the agglomeration of graphene sheets to produce graphene materials with a high SSA. For example, by activation with $Ni(NO_3)_2 \cdot 6H_2O$, Li and his co-workers [35] reported the synthesis of the novel porous reduced graphene oxide (p-RGO) with exfoliated sheets, fabricated through means of hydrothermal assembly calcination. Additionally, the SSA of p-RGO-5 (5 was the mass ratio of Ni to GO applied) (S_{Micro} = 99.8 $m^2 \cdot g^{-1}$, S_{BET} = 462.7 $m^2 \cdot g^{-1}$, $S_{Langmuir}$ = 647.3 $m^2 \cdot g^{-1}$) was higher than RGO (S_{Micro} = 63.7 $m^2 \cdot g^{-1}$, S_{BET} = 291.3 $m^2 \cdot g^{-1}$, $S_{Langmuir}$ = 407.8 $m^2 \cdot g^{-1}$), while the p-RGO-5 presented a large specific capacitance of 253.8 $F \cdot g^{-1}$ at 1.0 $A \cdot g^{-1}$. Wang et al. [36] created a type of covalent organic framework (COF) in which the rich mesopores blocked the reunion of reduced graphene oxide (RGO). The influence of COF content on the specific capacitance of the COF/RGO hybrid was also studied by Wang and his co-workers. They found that the optimized RGO/COF-20 hybrid (20 wt% COF) afforded a gravimetric specific capacitance of 321 $F \cdot g^{-1}$ and a volumetric specific capacitance of 237 $F \cdot cm^{-3}$. Although the SSA of graphene electrode material has been improved, both chemical and physical methods undermine chemical stability and electrical conductivity, causing a reduction in cycle life and power density [37].

Another type of SC is the pseudocapacitor, which can mimic the behavior of EDLCs with energy storing and releasing through multiple fast and highly reversible processes of Faradic redox reactions on the electrode surface. The capacitive property relies on the porosity of the materials and insertion and desertion of ions at the electrode/electrolyte interface [38,39]. Compared with an EDLC, the specific capacitance of pseudocapacitors is higher; however, the cycling stability is lower because of volumetric change in the process of charging and discharging. Conductive polymers (CPs), metal sulfides, metal oxides, metal carbides, and metal nitrides are the most common pseudocapacitive materials, and CPs are representative electrode materials for pseudocapacitors. Among them, CPs are perhaps the most representative, exhibiting an excellent pseudocapacitive performance by a fast and reversible redox reaction [40]. However, this type of SC also has several limitations. For example, the most notable drawback is the rapid decayed cycle stability when it is charged and discharged; this is due primarily to considerable mechanical degradation (e.g., expanding and shrinking) and irreversible structural changes [41]. Meanwhile, due to their dense structure, CPs, which only contact the electrolyte in a limited nature, suffer from a poor power density.

In order to overcome the drawbacks of EDCLs and pseudocapacitors, many studies have managed to fabricate new types of hybrid SCs by combining the above electrode materials (both carbonaceous materials and pseudocapacitive materials). In recent years, many CPs have been explored and used to manufacture CP/graphene composites in combination with graphene. The application of CP/graphene composites, such as SCs [42,43], solar cells [44], fuel cells [45], sensing platforms [46], etc., has also been investigated, and the application in SCs has aroused great interest among researchers due to the excellent electrochemical property of CP/graphene composites. These CP/graphene SC electrodes, which are supposed to combine the advantages of both CPs and graphene, show significant improvements on their capacitance performance and cyclic stability. Thus, the disadvantage of CP-only electrodes is effectively ameliorated.

Several reviews [18,47] concerning the synthesis methods and capacitive performance of graphene/CP hybrid SCs are available in the literature; however, most of these papers only focus on the relatively simple binary composites of graphene (and its derivatives) and CPs. In this review, apart from the widely considered binary CP/graphene composite electrodes for SCs, the most recent research progress of more sophisticated ternary and even quaternary composites from the past 5 years is also presented, offering valuable instruction for the selection and combination of promising electrode materials. Specifically, the content is divided into five sections. Section 1 introduces the properties of graphene and CPs and their application in the field of SCs. Section 2 discusses binary graphene/CP composites (PANI, PPy, and Pind) used for electrodes. Section 3 discusses ternary composites synthesized by combining graphene/CP composites with another material. In Section 4, the synthesis strategies and performance of quaternary composites are discussed. Finally, in Section 5, future perspectives on SC electrodes based on CP/graphene composites are also proposed.

2. Binary Composites

Binary composite refers to a material composed of two elements, parts, or divisions, including metal materials, non-metal materials, organic materials, polymer composite materials, etc. Binary composites, which are composed of CPs and graphene, exhibit higher stability and higher electrical conductivity than individual components due to the positive synergistic affection between CPs and graphene [47].

2.1. Graphene/PANI Composites

Polyaniline (PANI) is a promising conductive polymer that exhibits excellent electrochemical activity, environmental stability, and fast Faraday reactivity [48,49]. Many synthesis methods of PANI have been developed in recent decades, such as electrochemical polymerization and oxidative polymerization [50,51]. Apart from the level and type of dopant used, it is well known that the synthesis method adopted also has a significant effect on the electrochemical properties and the electrical conductivity of PANI [52].

PANI/graphene nanocomposites can be synthesized via different procedures such as interfacial polymerization [53], chemical polymerization techniques [51,54], and electrochemical polymerization [55]. In the process of synthesis, graphene can create a suitable environment for PANI growth. Zhao et al. [54] reported the synthesis of PANI/graphene nanocomposites fabricated through in situ high gravity chemical oxidative polymerization means in a rotating packed bed (RPB). Meanwhile, they found that the ammonium persulfate/aniline mole ratio, graphene dosage, reactor type, and aniline concentration play important roles in their morphology and electrochemical performance. A simple in situ chemical oxidative pathway was used to synthesize nanocomposites of PANI with GO in an acidic environment of aqueous sulfuric acid, while dodecylbenzene sulfonic acid (DBSA) was used as a surfactant and dopant [56]. The GO was synthesized from graphite through a modified Hummers method. Gul et al. [56] also studied the influence of different GO concentrations on the composite morphologies (as shown in Figure 1). It can clearly be observed from these images that GO is introduced into composites due to the changes in morphology, and extremely porous nanostructures with distributed nanofibers

are developed at 6% of GO (Figure 1e). DBSA is helpful for the constant growth of PANI on the surface of GO sheets during polymerization. As the GO concentration increases, the specific capacitance of the composite increases, reaching a maximum of 658 F g^{-1} at 6% of GO; it then decreases further (PANI: 158 F·g^{-1}, PANI–GO-1: 323 F·g^{-1}, PANI–GO-2: 345 F·g^{-1}, PANI–GO-4: 417 F·g^{-1}, PANI–GO-6: 658 F·g^{-1}, PANI–GO-8: 387 F·g^{-1}, PANI–GO-10: 355 F·g^{-1}). The largest average pore volume (0.037 cc·g^{-1}) and BET surface area (m^2·g^{-1}), as well as the smallest pore radius (14.561 Å), of PANI–GO-6 seem to be the reasons for the highest specific capacitance.

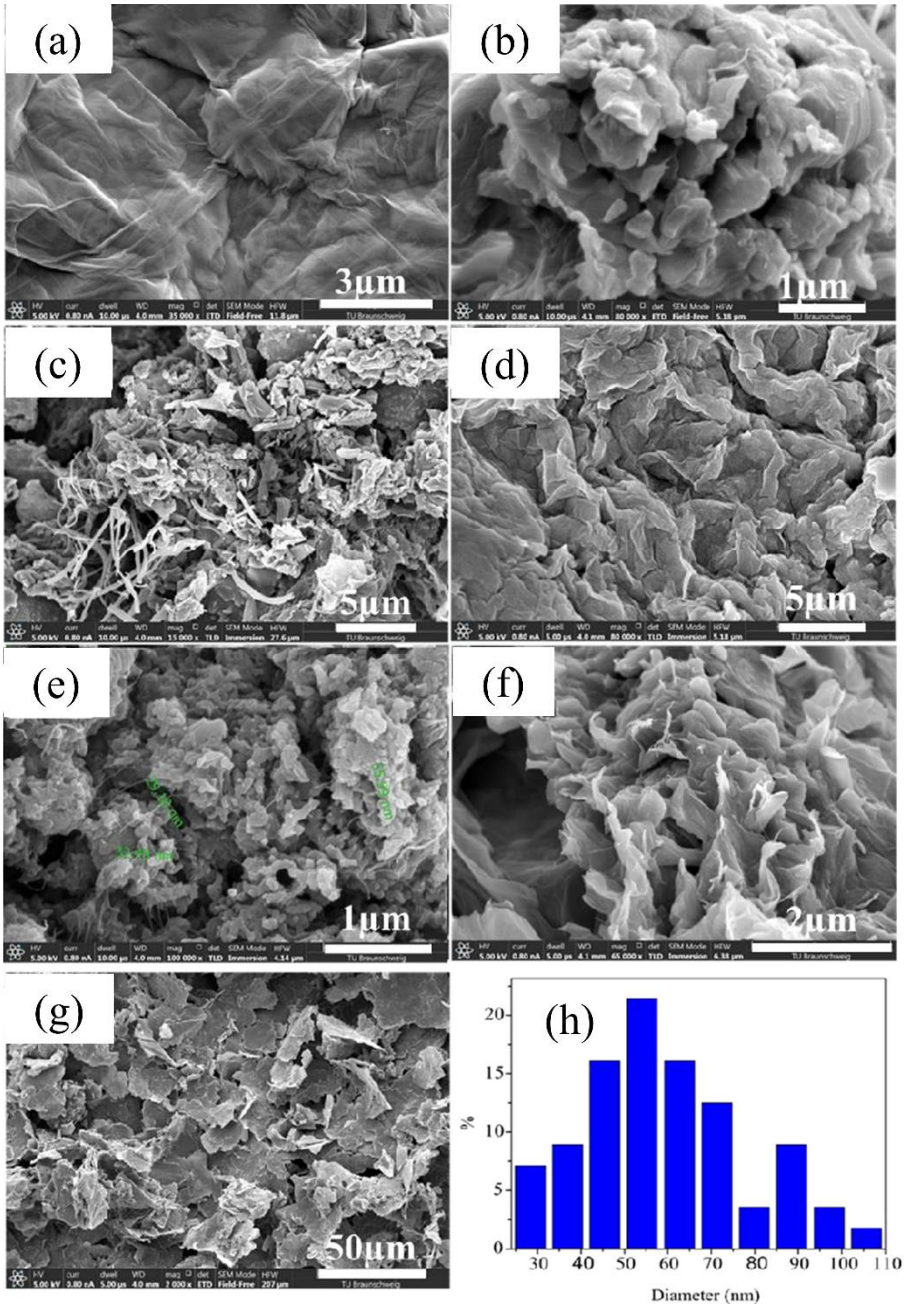

Figure 1. Scanning electron microscopy of electrode surfaces containing (**a**) graphene, (**b**) PANI, (**c**) PANI–GO-1, (**d**) PANI–GO-4, (**e**) PANI–GO-6, (**f**) PANI–GO-8, and (**g**) PANI–GO-10, and (**h**) particle size distribution histogram of PANI–GO-10 (Reprinted from ref. [56]).

Many studies have been conducted in recent years using RGO to replace GO as the electrode material of SCs due to the former's greater conductivity [57,58]. In general, RGO

is obtained from GO and then used to compound with PANI. The capacitance properties of RGO/PANI nanocomposites are greatly affected by changing the sequence of compositing or reducing GO and the electrolytes. Moyseowicz et al. [59] synthesized GO from graphite by a modified Hummers method. Then, the GO was reduced via hydrothermal treatment at 180 °C for 12 h in a stainless-steel autoclave while adding PANI into GO compared with the absence of PANI. The specific capacitance values of PANI, RGO-HT (RGO by hydrothermal treatment), and PANI/RGO-HT were 440, 236, and 420 $F \cdot g^{-1}$, respectively, at a current density of 0.2 $A \cdot g^{-1}$. The specific capacitance value of PANI/RGO-HT was 239 $F \cdot g^{-1}$, while PANI was 84 $F \cdot g^{-1}$ at a current density of 20 $A \cdot g^{-1}$. Meanwhile, the composite cyclic stability of PANI/RGO-HT was greatly improved, and the capacity retention rate remained at 80% after 6000 cycles compared with 46% of PANI after just 1000 cycles at a current density of 2 $A \cdot g^{-1}$.

2.2. Graphene/PPy Composites

Polypyrrole (PPy) is another important CP with a high theoretical capacitance of 620 $F \cdot g^{-1}$ [60]. Due to its appealing characteristics, such as excellent flexibility, low cost, sizeable energy density [61,62], high cycling stability [63], and quick charge/discharge process [64], PPy can be used to manufacture flexible electronic devices, such as wearable sensors [65], smart textiles [66], and roll-up displays [67]. Therefore, the important role of PPy in energy storage devices and electronic applications has attracted great attention from researchers. However, as with PANI, PPy also has poor cyclic stability. To alleviate this deficiency, researchers have synthesized graphene/PPy composites electrochemically or by polymerization.

Recently, Jia et al. [68] synthesized various PPy/GO films with different mass ratios by the confined polymerization inside the ice method. A prepared frozen pyrrole/GO layer and a mixture of adipic acid and ammonium were added into the mold, where the compound of deionized water and alcohol persulfate was initially added at a temperature of −20 °C. The reaction was carried out at −20 °C for 24 h. Additionally, the PPy/GO film was then obtained after thawing, washing, and drying. FSC-1, FSC-2, FSC-3, FSC-4, and FSC-5 were the flexible symmetrical SCs made of PPy, PPy/GO-1.0, PPy/GO-1.5, PPy/GO-2.0, and PPy/GO-2.5. Figure 2 shows that the CV curves of FSC devices (FSC-1, FSC-2, FSC-3, FSC-4, FSC-5) at different scan rates are closer to rectangles and are more symmetrical; the area of CV curves of FSC-5 is the largest, and FSC-5 exhibits a comparatively low ESR of 4.12 Ω (FSC-1: 22.4 Ω, FSC-2: 15.23 Ω, FSC-3: 11.11 Ω, FSC-4: 8.84 Ω). This study showed that, with the increase in GO content, the capacitance and electrical conductivity of SCs increased.

Using hexadecylpyridinium chloride (CPC) as a modifier of GO, Feng et al. [69] synthesized polypyrrole/modified graphite oxide (PPy/MGO) composites via in situ polymerization. CPC contains hydrophobic groups (pyridine rings), which combine with PPy chains and then interact on the surface of GO via π–π stacking. As a result, the specific capacitance of PPy/MGO (202 $F \cdot g^{-1}$) was higher than PPy/GO (137 $F \cdot g^{-1}$), and the capacitance utilization of PPy in PPy/MGO (183 $F \cdot g^{-1}$) was also higher than PPy/GO (129 $F \cdot g^{-1}$), indicating that the modification of GO could improve the performance of PPy/GO composites.

Ghanbari et al. [70] put GO powder into a microwave oven to exfoliate and reduce graphene oxide by microwave irradiation (MRGO), and then in situ polymerized pyrrole onto it. The specific capacitance of the reduced-graphene oxide/polypyrrole nanofiber (RGO/PPy-Nf) nanocomposite was 277 $F \cdot g^{-1}$ at a 1 $A \cdot^{-1}$ current density in a solution electrolyte containing 1 M H_2SO_4. The study showed that both mechanisms of EDLCs and faradaic reactions played an important role in the RGO/PPy-Nf nanocomposite.

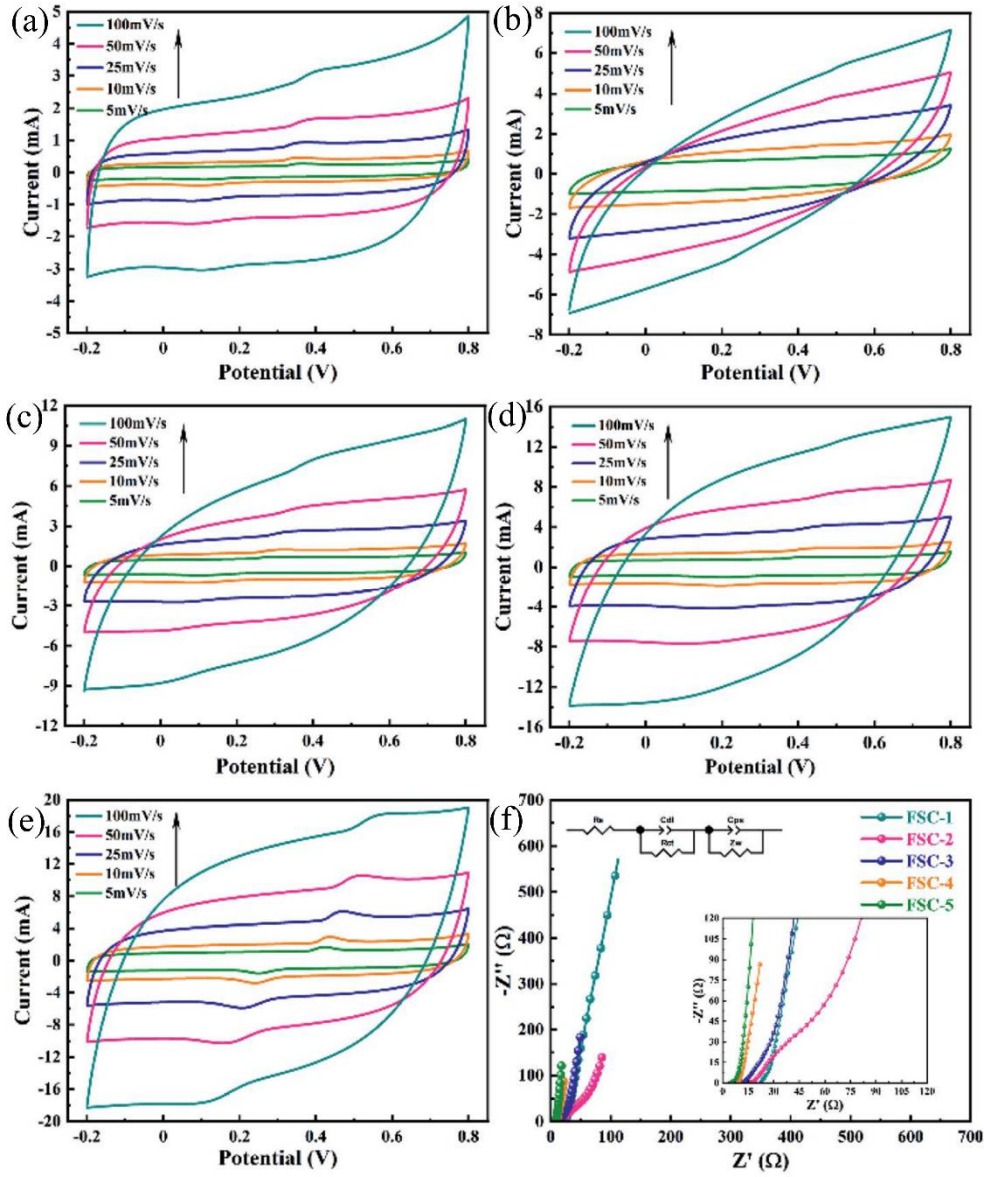

Figure 2. The CV behaviors of solid-state SCs at different scan rates: (**a**) FSC-1, (**b**) FSC-2, (**c**) FSC-3, (**d**) FSC-4, and (**e**) FSC-5. (**f**) Nyquist plots of the FSC devices (Reprinted from ref. [68]).

2.3. Graphene/Pind Composites

Recently, some researchers have demonstrated that polyindole (Pind) is a promising CP for the manufacture of SCs. The properties of Pind are similar to poly (paraphenylene) and PPy due to its special molecular structure containing a six-membered benzene ring fused in a five-membered pyrrole ring [71]. The synthesis methods of Pind are put into practice via various polymerization routes, such as electrochemical polymerization and chemical oxidative polymerization [72,73]. Pind shows a competitive redox potential compared to PPy and a slower hydrolytic degradation than PANI [74]. However, the conductivity of Pind is much lower than PPy and PANI (two orders of magnitude) [75]. In recent years, the application of Pind in electrode materials combined with graphene for SCs has attracted much attention.

Mudila et al. [76] synthesized various polyindole/graphene oxide (GO) nanocomposites (PINCs) with different concentrations of GO via a dilute solution polymerization method with the assistance of cetyltrimethylammonium bromide. This study showed that, with the increase in GO content, the thermal stability and the specific capacitance of PINCs increased regularly. For example, at a scan rate of 0.001 V/s, the specific capacitance of pure

polyindole was 21.89 F·g^{-1} compared to 399.97 F·g^{-1} PINCs with 20% *w*/*w* GO. In [77], the Pind/RGO nanocomposites, synthesized through a typical in situ chemical oxidative polymerization method, presented a high specific capacitance of 322.8 F·g^{-1} at 1.0 A·g^{-1}, and the cyclic stability decreased by only 5.5% after 1000 cycles. The above research provides evidence that the combination of Pind and graphene can improve the electrochemical utilization of Pind and the structural stability of graphene/Pind composites in the process of charging and discharging; therefore, specific capacitance and cycle stability have both been improved.

2.4. Comparison and Summary

PANI, PPy, and Pind are perceived as highly promising conductive polymers for hybrid SCs due to their large energy density, high conductivity, and eco-friendly and cheap features. There is little difference in environmental and electrochemical stability between these CPs (PANI, PPy, and Pind); however, the conductivity comparison of them follows the order of PPy > PANI > Pind [75,78].

The recent development of graphene and CP (PANI, PPy, and Pind) composites for SCs is summarized in Table 1. The electrochemical properties (i.e., charge/discharge speed, specific capacitance, and cycling stability) of graphene/CP composites are affected by many factors, such as concentrations of graphene and its derivatives, properties of individual CPs, and polymerization methods. Moreover, the combination of CPs and graphene greatly enhances the electrochemical properties of graphene/CP composites, showing excellent synergy between CPs and graphene and its derivatives [79].

Table 1. Performance of the SCs based on graphene/CP composites.

Materials	Electrolyte	Testing	Capacitance	Capacitance Retention	Year	References
PANI	PVA/H_3PO_4	Two-electrode	283 F g^{-1} at 0.5 A g^{-1}	-	2013	[80]
PANI/graphene	1 M H_2SO_4		408 F g^{-1} at 5 mV s^{-1}	84% after 40 cycles	2009	[81]
PANI/GO	0.5 M H_2SO_4	Three-electrode	448 F g^{-1} at 0.5 A g^{-1}	81% after 5000 cycles	2014	[82]
PANI/RGO-HT	1 M H_2SO_4	Three-electrode	420 F g^{-1} at 0.2 A g^{-1}	80% after 6000 cycles	2018	[59]
PANI/GO	1.1 M H_2SO_4	Three-electrode	658 F g^{-1} at 10 A g^{-1}	84.09% after 2000 cycles	2019	[56]
PPy	PVA/H_3PO_4	Two-electrode	170 F g^{-1} at 0.5 A g^{-1}	-	2014	[83]
PPy/graphene	1 M NaCl		165 F g^{-1} at 1 A g^{-1}	-	2010	[84]
PPy/GO	PVA/H_3PO_4	Three-electrode	97.3 mF cm^{-2} at 1 mA cm^{-2}	94% after 1000 cycles	2020	[68]
PPy/MGO	2 M $NaNO_3$	Three-electrode	202 F g^{-1} at 1 A g^{-1}	83.8% after 1000 cycles	2013	[69]
PPy/GO	2 M $NaNO_3$	Three-electrode	137 F g^{-1} at 1 A g^{-1}	-	2013	[69]
EG-RGO/PPy	1 M H_2SO_4	Three-electrode	420 F g^{-1} at 0.5 A g^{-1} 240 F g^{-1} at 5 A g^{-1}	93% after 200 cycles at 1 A g^{-1}	2013	[85]
RGO/PPy-Nf	1 M H_2SO_4	Two-electrode	277 F g^{-1} at 1 A g^{-1}	95% after 1000 cycles	2021	[70]
Pind	1 M H_2SO_4	Three-electrode	112 F g^{-1} at 1 A g^{-1}	82.3% after 5000 cycles at 10 A g^{-1}	2017	[86]
Pind/GO	1 M KOH	Three-electrode	399.97 F g^{-1} at 1 mV S^{-1}	99% after 50 cycles at 0.1 V S^{-1}	2015	[76]
Pind/RGO	1 M H_2SO_4	Three-electrode	322.8 F g^{-1} at 1 A g^{-1}	94.5% after 1000 cycles	2016	[77]
Pind/RGO	1 M $HClO_4$	Three-electrode	214 F g^{-1} at 5 A g^{-1}	62% after 5000 cycles	2020	[87]

3. Ternary Composites

The binary composites of CPs with graphene and its derivatives have proved to have higher electrochemical properties than their individual components. Inspired by this, researchers have conducted plenty of work to improve the electrochemical performance of graphene/CP composites used in SCs by combining them with another material, such as metal sulfides, metal oxides, and nonmetal oxides, to form a ternary composite material.

Wang and his co-workers [88] fabricated a ternary composite SiO_2/graphene/PANI (SGP) as the SC electrode material. In the study, hydrophilic SiO_2 was used as an inorganic porous framework layer to bridge PANI and graphene, which not only inhibited the accumulation between graphene and PANI and graphene layers, but also improved ion exchanges and the interactions at the electrolyte/electrode interface. Although the conduc-

tivity of SiO_2 is poor, the excellent synergy between SiO_2, graphene, and PANI improved the specific capacitance of SGP-1 composites (727.0 $F \cdot g^{-1}$) compared with SiO_2/graphene (88.8 $F \cdot g^{-1}$), graphene (108.0 $F \cdot g^{-1}$), and graphene/PANI (302.1 $F \cdot g^{-1}$); meanwhile, the capacitance retention rate of SGP-4 was 90% after 3500 cycles.

Xu et al. [89] synthesized ZnS/RGO/CP composites by doping with the same mass ratio of CPs (PANI, PPy, polythiophene (PTh), poly 3,4-ethylenedioxythiophene (PEDOT)) on the surface of a ZnS/RGO composite through an in situ polymerization method. Meanwhile, in comparison with other ZnS/RGO/CP composites (PPy, PTh, PEDOT), the capacitance performance and cycle stability of ZnS/RGO/PANI were the best. The specific capacitance of ZnS/RGO/PANI was 722.0 and 1045.3 $F \cdot g^{-1}$ at 1 $A \cdot g^{-1}$ in a two-electrode and three-electrode system, higher than 613.8 and 787 $F \cdot g^{-1}$ of ZnS/RGO/PPy, and the cycle stability of ZnS/RGO/PANI was 76.1% and 160% in a two-electrode and three-electrode system after 1000 loops, which was also higher than 50% and 149% of ZnS/RGO/PPy.

Ramesh et al. [90] synthesized Co_3O_4@NGO/Pind composites by hydrothermal treatment after ultrasonication, and the synthesis process is shown in Figure 3. Figure 4 shows that the electrochemical performances of Co_3O_4@NGO/Pind composites were researched through galvanostatic charge–discharge (GCD), cyclic voltammetry (CV), and an electrochemical impedance spectroscopy analysis (EIS) method. The study indicated that the specific capacitance of Co_3O_4@NGO/Pind was ~680 $F \cdot g^{-1}$ at 0.5 $A \cdot g^{-1}$, and the capacitance retention rate was 96% after 3000 cycles. Despite the fact that Co_3O_4@NGO/Pind exhibited great electrochemical performance, it was unable to represent the ideal capacitive behavior due to the unsymmetrical profiles on CV and non-triangular shapes on GCD. These could be attributed to the addition of multiple compounds and compatibility difference. Hence, further research is necessary to overcome such drawbacks to improve the capacitor properties.

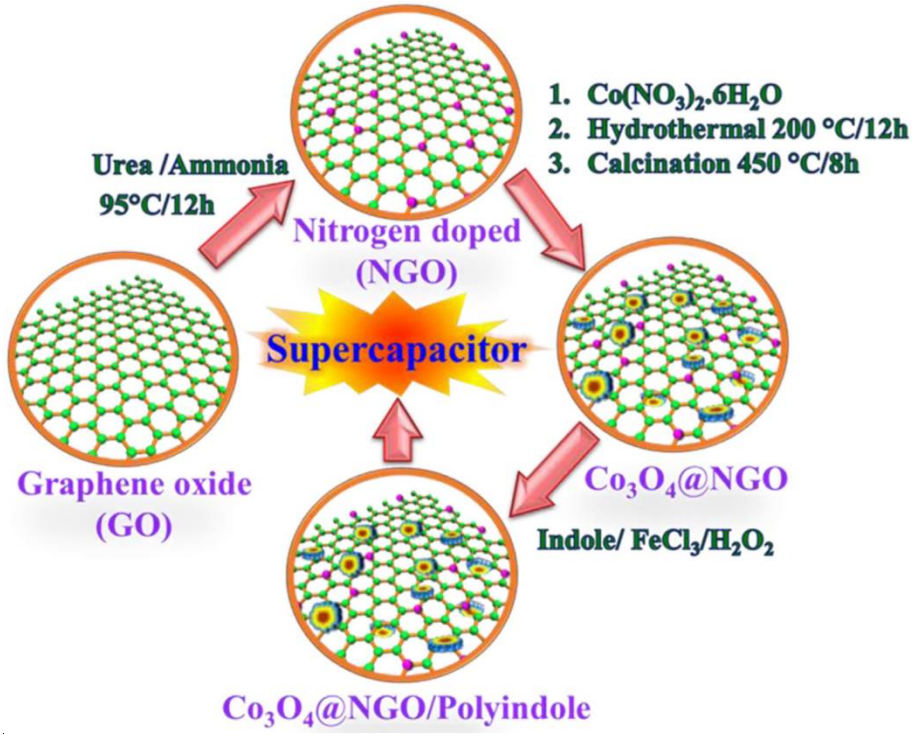

Figure 3. Schematic representation for the synthesis of Co_3O_4@NGO and Co_3O_4@NGO/Pind composites (Reprinted from ref. [90]).

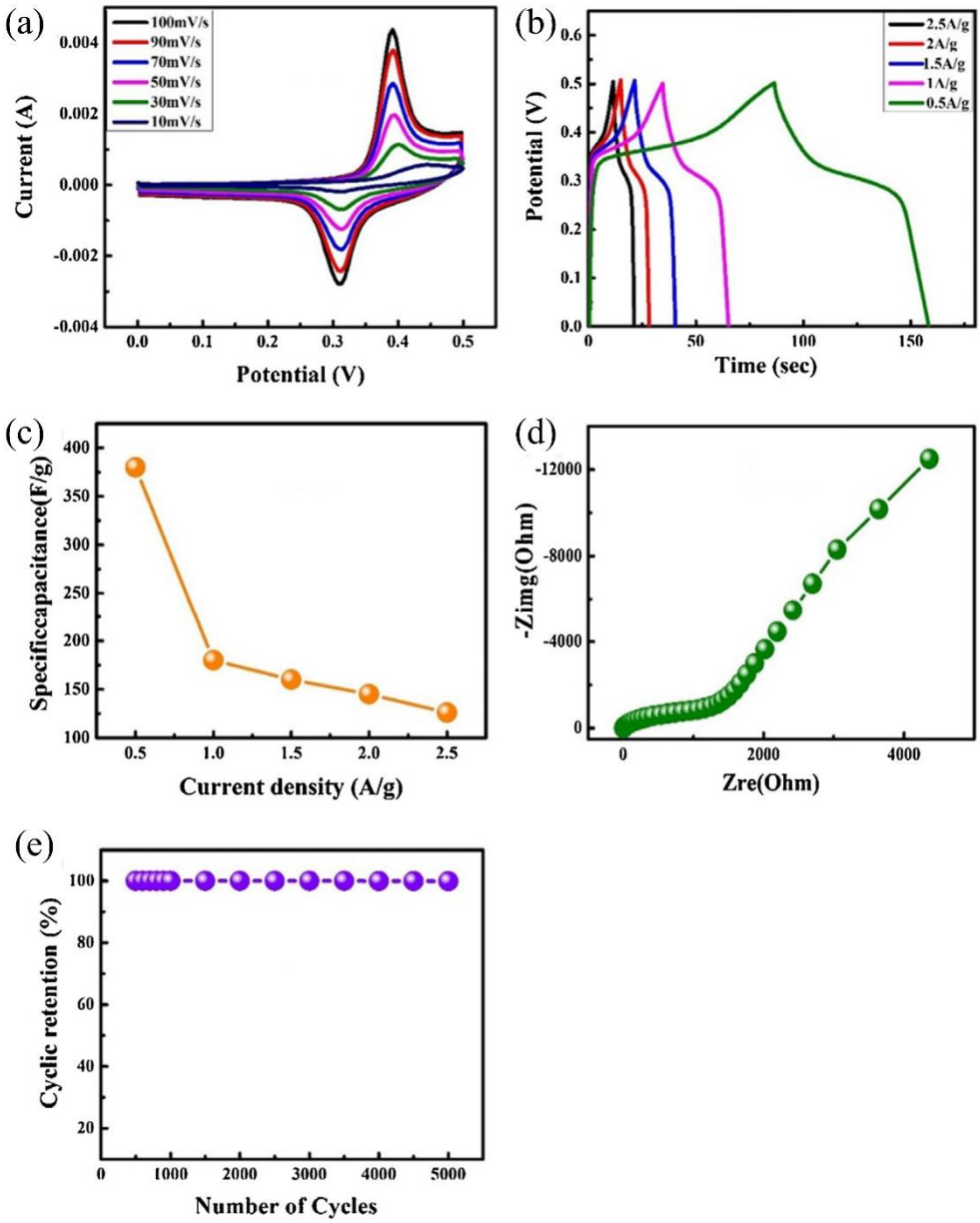

Figure 4. Electrochemical performance of (**a**) CV, (**b**) GCD, (**c**) current density vs. specific capacitance, (**d**) EIS, and (**e**) cyclic stability of Co_3O_4@NGO/Pind composite. Reprinted from ref. [90].

The recent development of ternary composites (graphene and its derivatives, CPs, and other materials) for SCs is summarized in Table 2. Compared with binary composites, ternary composites exhibit better electrochemical performance; this is due not only to the synergy between CPs, graphene and its derivatives, and other materials, but also to the increase in SSA that results in a reduction in diffusive path length [91]. In addition, ternary composites of graphene, metal oxides, and CPs can prevent the detachment of metal oxide nanoparticles and improve cycling stability [92]. Ternary composite metals and metal oxides, or sulfides, are the commonly used materials in graphene/CP composites to form ternary composites due to their superior conductivity and pseudocapacitance. Therefore, the improvement in electrochemical performance by adding nonmetallic material (poor conductivity) into graphene/CP composites primarily promotes interfacial interactions [88].

Table 2. Electrochemical performance of some previously reported ternary composites.

Materials	Electrolyte	Testing	Capacitance	Capacitance Retention	Year	References
GO/Pt/DBSA-PANI	1 M H_2SO_4	Three-electrode	227.2 F g^{-1} at 0.9 mV S^{-1}	96% after 1500 cycles	2019	[93]
ZnS/RGO/PANI	6 M KOH	Two-electrode	722 F g^{-1} at 1 A g^{-1}	76.1% after 1000 cycles	2020	[89]
ZnS/RGO/PPy	6 M KOH	Two-electrode	613.8 F g^{-1} at 1 A g^{-1}	50% after 1000 cycles	2020	[89]
NiO/Gr/PPy	6 M KOH	Three-electrode	970.85 F g^{-1} at 1 A g^{-1}	-	2020	[94]
RGO/Pind/gammer-Al_2O_3	1.0 M $HClO_4$	Three-electrode	308 F g^{-1} at 5 A g^{-1}	83% after 5000 cycles	2020	[87]
Co_3O_4@NGO/polyindole	2 M KOH	Three-electrode	~680 F g^{-1} at 0.5 A g^{-1}	96% after 3000 cycles	2020	[90]
TiO_2@PPy/rGO	2 M KOH	Three-electrode	462.1 F g^{-1} at 0.5 A g^{-1}	70% after 1500 cycles	2021	[95]
SiO_2/graphene/PANI	1 M H_2SO_4	Three-electrode	727 F g^{-1}	90% after 3500 cycles	2021	[88]

4. Quaternary Composites

Based on the above research, it is clear that multiple components can make up for respective deficiencies and improve their comprehensive performance in relation to electrochemistry; quaternary composites of CPs with graphene are supposed to exhibit superior capacity and service life. A recent study showed that, by way of reduction in platinum nanoparticles into a modified PANI with carbon nanotubes (CNTs) and graphene nanosheets (GNS), a quaternary composite of PANI/GNS/CNT/Pt was synthesized [96]. The advantages of four materials—excellent electrical conductivity of GNS and CNTs, large surface area and conductivity of Pt nanoparticles, and high redox activity of PANI—were well presented in the quaternary electrode of PANI/GNS/CNT/Pt, which showed excellent synergy between PANI, GNS, CNTs, and Pt.

Gottam et al. [97] synthesized a quaternary composite of MoO_3–MC–SiO_2–PANI through a chemical process using molybdenum oxide (MoO_3), mesoporous carbon (MC), silicon dioxide (SiO_2), and PANI materials. The study showed that the specific capacitance of the carbon substrate could be improved by adding SiO_2 into it to form MC–SiO_2, and the combination of the two materials of PANI and MoO_3 could form a dual charge storage redox action, which had the potential for excellent capacitive performance (see Figure 5).

Table 3 shows that the specific capacitance and cycle stability of the quaternary composite (PANI/GNS/CNT/Pt) were higher than the ternary composites (PANI/GNS/CNT, PANI/GNT/Pt, and PANI/GNS/Pt) in [96], and the specific capacitance of the quaternary composite (MoO_3–MC–SiO_2–PANI) was higher than that of ternary composites (MC–SiO_2–PANI and MoO_3–MC–SiO_2) in [97]. However, few studies have been performed on quaternary electrodes in recent years, and the study on the mechanism of quaternary composites is unclear, as quaternary composites involve four components. Therefore, more research on quaternary composites is needed to study their synthesis, electrochemical properties, and mechanism, which will provide the possibility for the creation of next-generation energy storage systems.

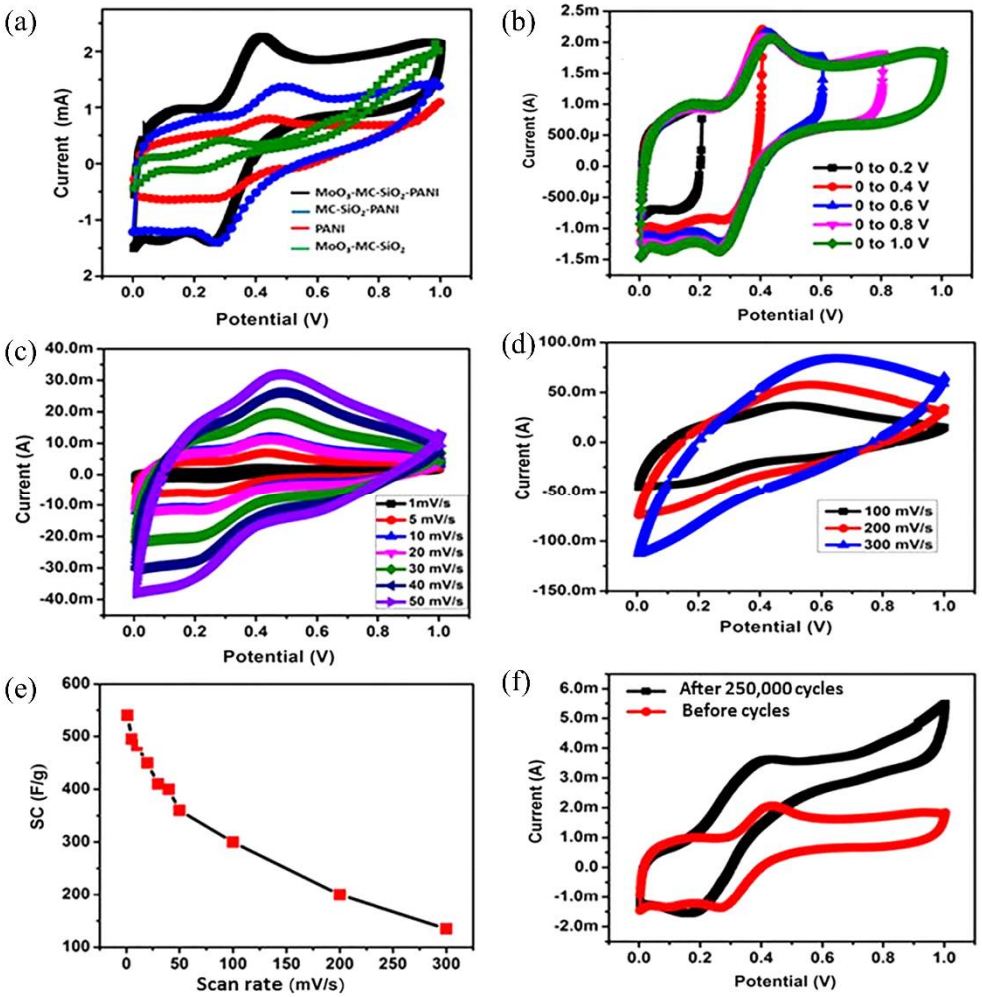

Figure 5. (**a**) CV curves of MoO_3–MC–SiO_2–PANI, MC–SiO_2–PANI, PANI, and MoO_3–MC–SiO_2 at 1 mV/s scan rate; (**b**) CV curves in different voltage ranges of MoO_3–MC–SiO_2–PANI at 1 mV/s scan rate; (**c**,**d**) CV of MoO_3–MC–SiO_2–PANI at different scan rates from 1 to 300 mV/s; (**e**) scan rate vs. specific capacitance of MoO_3–MC–SiO_2–PANI; (**f**) CV of MoO_3–MC–SiO_2–PANI at 1 mV/s before and after 250,000 CD cycles. Reprinted with permission from ref [97]. Copyright 2021 John Wiley and Sons.

Table 3. Electrochemical performance of the two quaternary composites.

Materials	Electrolyte	Testing	Capacitance	Capacitance Retention	Year	References
PANI/GNS/CNT/Pt	1 M H_2SO_4	Two-electrode	3450 C g^{-1} at 4.0 μA S^{-1}	84.8% after 1000 cycles	2017	[96]
PANI/GNS/CNT	1 M H_2SO_4	Two-electrode	952 C g^{-1} at 4.0 μA S^{-1}	63% after 1000 cycles	2017	[96]
PANI/GNT/Pt	1 M H_2SO_4	Two-electrode	366 C g^{-1} at 4.0 μA S^{-1}	38.9% after 1000 cycles	2017	[96]
PANI/GNS/Pt	1 M H_2SO_4	Two-electrode	1123 C g^{-1} at 4.0 μA S^{-1}	36.3% after 1000 cycles	2017	[96]
MoO_3–MC–SiO_2–PANI	1 M H_2SO_4	Two-electrode	535 F g^{-1} at 1 mV S^{-1}	57% after 250,000 cycles at 16.6 A g^{-1}	2021	[97]
MC–SiO_2–PANI	1 M H_2SO_4	Two-electrode	410 F g^{-1} at 1 mV S^{-1}	-	2021	[97]
MoO_3–MC–SiO_2	1 M H_2SO_4	Two-electrode	80 F g^{-1} at 1 mV S^{-1}	-	2021	[97]

5. Summary and Outlook

Carbon materials, metal oxides, and CPs are three generally studied electrode materials for SCs. Metal oxides have a higher specific capacity, but their low conductivity, high cost, and pollution to the environment are limitations for their application in SCs. Graphene is one of the ideal SC materials due to its superior electrochemical properties (such as high electrical conductivity) and highly specific surface area. However, because of the effect of van der Waals interaction, the accumulation of graphene sheets decreased the specific capacitance of graphene electrodes [30,31]. CPs could probably become next-generation SC electrode materials due to their low cost and high pseudocapacitance. However, pure CP electrodes expand and shrink during charging and discharging, resulting in low cycle stability [41]. Nevertheless, with the combination of graphene and CPs, the newly formed graphene/CP composites have the advantages of high specific capacitance and excellent cycle stability, making them a more promising candidate for SC electrode materials.

In this review, we have discussed several graphene/CP composites (PANI, PPy, and Pind) and their potential applications in SCs. The methods of synthesis for electrode materials, including the one-pot synthesis route [56], hydrothermal-assisted synthesis method [59], and ice-interface assisted synthesis method [68], are discussed in this article. Meanwhile, the electrochemical performances of pure, binary, ternary, and quaternary composites have been discussed and compared. EDLCs and pseudocapacitors composed of pure electrode materials have the disadvantage of poor cyclic stability or low specific capacitance, while hybrid SCs composed of binary, ternary, and quaternary composites store energy through Faradic redox reactions and charge accumulation at the electrode/electrolyte interface. The factors affecting SCs are as follows: the interfacial interaction between graphene and CPs, the properties of CPs, the microstructure of composites, etc. [98]. Therefore, researchers have conducted many studies to improve the interfacial interaction between graphene and CPs and the microstructure of composites by adding one more material to form ternary composite electrode materials, and even quaternary composite electrode materials, to further enhance this effect.

In conclusion, graphene/CP composites are superior materials in the application of SCs. Great progress has been achieved with the unremitting efforts of researchers for better electrochemical performance of electrode materials. However, the following questions remain to be addressed by researchers in this field.

First, compared with other carbon materials, such as coconut-shell-activated carbon, the cost of graphene is still high. New techniques for the synthesis of graphene with a low cost and high quality still need to be developed. At present, the electrochemical performance of CPs cannot meet the requirement of large-scale commercial applications, and the synthesis of new CPs also requires development by researchers.

Second, during the processes of synthesizing graphene/CP composites, the high SSA of graphene should be maintained. New techniques for uniformly mixing graphene into CPs need to developed to prevent the restacking of graphene.

Third, the application of binary composites, ternary composites, and quaternary composites of graphene/CP in SCs has proven to be very successful; however, the mechanisms used to explain the synergy between CPs, graphene, and other materials are not clear. Thus, more mechanisms need to be studied to optimize the compositions and morphologies of graphene/CP composites. We believe that graphene/CP composites with higher electrochemical performance can be found thanks to the pursuit of researchers who might finally realize their application in commercial fields.

Author Contributions: X.C. and X.J. conceived the idea. X.C. prepared an initial draft of the manuscript. X.C., Y.Q., K.S. and X.J. have participated in the writing of the final manuscript, and agreed to the published version of the manuscript. All authors have read and agreed to the published version of the manuscript.

Funding: The financial support for this work provided by the Fundamental Research Funds for the Central Universities (WUT:2020IVA022) is gratefully acknowledged.

Institutional Review Board Statement: Not applicable.

Informed Consent Statement: Not applicable.

Data Availability Statement: Not applicable.

Conflicts of Interest: The authors declare no conflict of interest.

References

1. Zhao, S.; Zhao, Z.; Yang, Z.; Ke, L.; Kitipornchai, S.; Yang, J. Functionally graded graphene reinforced composite structures: A review. *Eng. Struct.* **2020**, *210*, 110339. [CrossRef]
2. Xia, C.; Shahedi Asl, M.; Sabahi Namini, A.; Ahmadi, Z.; Delbari, S.A.; Le, Q.V.; Shokouhimehr, M.; Mohammadi, M. Enhanced fracture toughness of ZrB_2–SiCw ceramics graphene nano-platelets. *Ceram. Int.* **2020**, *46*, 24906–24915. [CrossRef]
3. Vajdi, M.; Moghanlou, F.S.; Nekahi, S.; Ahmadi, Z.; Motallebzadeh, A.; Jafarzadeh, H.; Asl, M.S. Role of graphene nano-platelets on thermal conductivity and microstructure of TiB_2-SiC ceramics. *Ceram. Int.* **2020**, *46*, 21775–21783. [CrossRef]
4. Tajik, S.; Dourandish, Z.; Zhang, K.; Beitollahi, H.; Le, Q.V.; Jang, H.W.; Shokouhimehr, M. Carbon and graphene quantum dots: A review on syntheses, characterization, biological and sensing applications for neurotransmitter determination. *RSC Adv.* **2020**, *1*, 15406–15429. [CrossRef]
5. Jiao, D.; Zheng, A.; Liu, Y.; Zhang, X.; Wang, X.; Wu, J.; She, W.; Lv, K.; Cao, L.; Jiang, X. Bidirectional differentiation of BMSCs induced by a biomimetic procallus based on a gelatin-reduced graphene oxide reinforced hydrogel for rapid bone regeneration. *Bioact. Mater.* **2021**, *6*, 2011–2028. [CrossRef] [PubMed]
6. Wang, H.; Mi, X.; Li, Y.; Zhan, S. 3D Graphene-Based Macrostructures for Water Treatment. *Adv. Mater.* **2019**, *32*, 1806843. [CrossRef]
7. Katubi, K.M.M.; Alsaiari, N.S.; Alzahrani, F.M.; M Siddeeg, S.; A Tahoon, M. Synthesis of Manganese Ferrite/Graphene Oxide Magnetic Nanocomposite for Pollutants Removal from Water. *Processes* **2021**, *9*, 589. [CrossRef]
8. Du, Y.; Xiao, P.; Yuan, J.; Chen, J. Research Progress of Graphene-Based Materials on Flexible Supercapacitors. *Coatings* **2020**, *10*, 892. [CrossRef]
9. Kumar, R.; Sahoo, S.; Joanni, E.; Singh, R.K.; Maegawa, K.; Tan, W.K.; Kawamura, G.; Kar, K.K.; Matsuda, A. Heteroatom doped graphene engineering for energy storage and conversion. *Mater. Today* **2020**, *39*, 47–65. [CrossRef]
10. Palmieri, V.; Papi, M. Can graphene take part in the fight against COVID-19? *Nano Today* **2020**, *33*, 100883. [CrossRef]
11. Seifi, T.; Reza Kamali, A. Antiviral performance of graphene-based materials with emphasis on COVID-19: A review. *Med. Drug Discov.* **2021**, *11*, 100099. [CrossRef] [PubMed]
12. Yang, W.; Ni, M.; Ren, X.; Tian, Y.; Li, N.; Su, Y.; Zhang, X. Graphene in Supercapacitor Applications. *Curr. Opin. Colloid Interface Sci.* **2015**, *20*, 416–428. [CrossRef]
13. Wang, B.; Ruan, T.; Chen, Y.; Jin, F.; Peng, L.; Zhou, Y.; Wang, D.; Dou, S. Graphene-based composites for electrochemical energy storage. *Energy Storage Mater.* **2020**, *24*, 22–51. [CrossRef]
14. Huang, Z.; Li, L.; Wang, Y.; Zhang, C.; Liu, T. Polyaniline/graphene nanocomposites towards high-performance supercapacitors: A review. *Compos. Commun.* **2018**, *8*, 83–91. [CrossRef]
15. Chen, S.; Qiu, L.; Cheng, H. Carbon-Based Fibers for Advanced Electrochemical Energy Storage Devices. *Chem. Rev.* **2020**, *120*, 2811–2878. [CrossRef] [PubMed]
16. Liu, L.; Zhao, H.; Lei, Y. Review on Nanoarchitectured Current Collectors for Pseudocapacitors. *Small Methods* **2019**, *3*, 1800341. [CrossRef]
17. Seman, R.N.A.R.; Azam, M.A.; Ani, M.H. Graphene/transition metal dichalcogenides hybrid supercapacitor electrode: Status, challenges, and perspectives. *Nanotechnology* **2018**, *29*, 502001. [CrossRef]
18. Wang, M.; Xu, Y. Design and construction of three-dimensional graphene/conducting polymer for supercapacitors. *Chin. Chem. Lett.* **2016**, *27*, 1437–1444. [CrossRef]
19. Wang, Y.; Xia, Y. Recent Progress in Supercapacitors: From Materials Design to System Construction. *Adv. Mater.* **2013**, *25*, 5336–5342. [CrossRef] [PubMed]
20. Jung, S.; Myung, Y.; Das, G.S.; Bhatnagar, A.; Park, J.; Tripathi, K.M.; Kim, T. Carbon nano-onions from waste oil for application in energy storage devices. *New J. Chem.* **2020**, *44*, 7369–7375. [CrossRef]
21. Thirumal, V.; Dhamodharan, K.; Yuvakkumar, R.; Ravi, G.; Saravanakumar, B.; Thambidurai, M.; Dang, C.; Velauthapillai, D. Cleaner production of tamarind fruit shell into bio-mass derived porous 3D-activated carbon nanosheets by CVD technique for supercapacitor applications. *Chemosphere* **2021**, *282*, 131033. [CrossRef]
22. Yang, Z.; Tian, J.; Yin, Z.; Cui, C.; Qian, W.; Wei, F. Carbon nanotube- and graphene-based nanomaterials and applications in high-voltage supercapacitor: A review. *Carbon* **2019**, *141*, 467–480. [CrossRef]
23. Peigney, A.; Laurent, C.; Flahaut, E.; Bacsa, R.R.; Rousset, A. Specific surface area of carbon nanotubes and bundles of carbon nanotubes. *Carbon* **2001**, *39*, 507–514. [CrossRef]
24. Kim, J.; Shin, Y.; Lee, J.; Bae, E.; Jeon, Y.; Jeong, C.; Yun, M.; Lee, S.; Han, D.; Huh, J. The Effect of Reduced Graphene Oxide-Coated Biphasic Calcium Phosphate Bone Graft Material on Osteogenesis. *Int. J. Mol. Sci.* **2017**, *18*, 1725. [CrossRef] [PubMed]
25. Ban, F.Y.; Majid, S.R.; Huang, N.M.; Lim, H.N. Graphene Oxide and Its Electrochemical Performance. *Int. J. Electrochem. Sci.* **2012**, *7*, 4345–4351.

26. Singh, V.; Joung, D.; Zhai, L.; Das, S.; Khondaker, S.I.; Seal, S. Graphene based materials: Past, present and future. *Prog. Mater. Sci.* **2011**, *56*, 1178–1271. [CrossRef]
27. Gao, Y.; Han, B.; Zhao, W.; Ma, Z.; Yu, Y.; Sun, H. Light-Responsive Actuators Based on Graphene. *Front. Chem.* **2019**, *7*, 506. [CrossRef] [PubMed]
28. Gadgil, B.; Damlin, P.; Kvarnstrom, C. Graphene vs. reduced graphene oxide: A comparative study of graphene-based nanoplatforms on electrochromic switching kinetics. *Carbon* **2016**, *96*, 377–381. [CrossRef]
29. Oh, H.M.; Kim, H.; Kim, H.; Jeong, M.S. Fabrication of Stacked MoS_2 Bilayer with Weak Interlayer Coupling by Reduced Graphene Oxide Spacer. *Sci. Rep.* **2019**, *9*, 5900. [CrossRef]
30. Zhang, X.; Zhang, H.; Li, C.; Wang, K.; Sun, X.; Ma, Y. Recent advances in porous graphene materials for supercapacitor applications. *RSC Adv.* **2014**, *4*, 45862–45884. [CrossRef]
31. El-Kady, M.F.; Strong, V.; Dubin, S.; Kaner, R.B. Laser Scribing of High-Performance and Flexible Graphene-Based Electrochemical Capacitors. *Science* **2012**, *335*, 1326–1330. [CrossRef] [PubMed]
32. Stoller, M.D.; Park, S.; Zhu, Y.; An, J.; Ruoff, R.S. Graphene-Based Ultracapacitors. *Nano Lett.* **2008**, *8*, 3498–3502. [CrossRef]
33. Nanaji, K.; Sarada, B.V.; Varadaraju, U.V.; Rao, T.N.; Anandan, S. A novel approach to synthesize porous graphene sheets by exploring KOH as pore inducing agent as well as a catalyst for supercapacitors with ultra-fast rate capability. *Renew. Energy* **2021**, *172*, 502–513. [CrossRef]
34. Yoon, Y.; Lee, K.; Kwon, S.; Seo, S.; Yoo, H.; Kim, S.; Shin, Y.; Park, Y.; Kim, D.; Choi, J.; et al. Vertical Alignments of Graphene Sheets Spatially and Densely Piled for Fast Ion Diffusion in Compact Supercapacitors. *ACS Nano* **2014**, *8*, 4580–4590. [CrossRef]
35. Li, P.; Li, H.; Zhang, X.; Zheng, X. Facile fabrication and improved supercapacitive performance of exfoliated graphene with hierarchical porous structure. *J. Energy Storage* **2021**, *33*, 102044. [CrossRef]
36. Wang, C.; Liu, F.; Chen, J.; Yuan, Z.; Liu, C.; Zhang, X.; Xu, M.; Wei, L.; Chen, Y. A graphene-covalent organic framework hybrid for high-performance supercapacitors. *Energy Storage Mater.* **2020**, *32*, 448–457. [CrossRef]
37. Raccichini, R.; Varzi, A.; Passerini, S.; Scrosati, B. The role of graphene for electrochemical energy storage. *Nat. Mater.* **2015**, *14*, 271–279. [CrossRef]
38. Fleischmann, S.; Mitchell, J.B.; Wang, R.C.; Zhan, C.; Jiang, D.E.; Presser, V.; Augustyn, V. Pseudocapacitance: From Fundamental Understanding to High Power Energy Storage Materials. *Chem. Rev.* **2020**, *120*, 6738–6782. [CrossRef] [PubMed]
39. Augustyn, V.; Simon, P.; Dunn, B. Pseudocapacitive oxide materials for high-rate electrochemical energy storage. *Energy Environ. Sci.* **2014**, *7*, 1597–1614. [CrossRef]
40. Subramanian, B.; Veerappan, M.; Rajan, K.; Chen, Z.; Hu, C.; Wang, F.; Wang, F.; Yang, M. Fabrication of Hierarchical Indium Vanadate Materials for Supercapacitor Application. *Glob. Chall.* **2020**, *4*, 2000002. [CrossRef]
41. González, A.; Goikolea, E.; Barrena, J.A.; Mysyk, R. Review on supercapacitors: Technologies and materials. *Renew. Sustain. Energy Rev.* **2016**, *58*, 1189–1206. [CrossRef]
42. Liu, G.; Shi, Y.; Wang, L.; Song, Y.; Gao, S.; Liu, D.; Fan, L. Reduced graphene oxide/polypyrrole composite: An advanced electrode for high-performance symmetric/asymmetric supercapacitor. *Carbon Lett.* **2020**, *30*, 389–397. [CrossRef]
43. Vannathan, A.A.; Kella, T.; Shee, D.; Mal, S.S. One-Pot Synthesis of Polyoxometalate Decorated Polyindole for Energy Storage Supercapacitors. *ACS Omega* **2021**, *6*, 11199–11208. [CrossRef]
44. Lee, B.H.; Lee, J.; Kahng, Y.H.; Kim, N.; Kim, Y.J.; Lee, J.; Lee, T.; Lee, K. Graphene-conducting polymer hybrid transparent electrodes for efficient organic optoelectronic devices. *Adv. Funct. Mater.* **2014**, *24*, 1847–1856. [CrossRef]
45. Yong, Y.; Dong, X.; Chan-Park, M.B.; Song, H.; Chen, P. Macroporous and monolithic anode based on polyaniline hybridized Three-dimensional graphene for high-performance microbial fuel cells. *ACS Nano* **2012**, *6*, 2394–2400. [CrossRef] [PubMed]
46. Hur, J.; Park, S.; Bae, J. Elaborate chemical sensors based on graphene/conducting polymer hybrids. *Curr. Org. Chem.* **2015**, *19*, 1117–1133. [CrossRef]
47. Shen, F.; Pankratov, D.; Chi, Q. Graphene-conducting polymer nanocomposites for enhancing electrochemical capacitive energy storage. *Curr. Opin. Electrochem.* **2017**, *4*, 133–144. [CrossRef]
48. Mo, Y.; Meng, W.; Xia, Y.; Du, X. Redox-Active Gel Electrolyte Combined with Branched Polyaniline Nanofibers Doped with Ferrous Ions for Ultra-High-Performance Flexible Supercapacitors. *Polymers* **2019**, *11*, 1357. [CrossRef]
49. Ajpi, C.; Leiva, N.; Vargas, M.; Lundblad, A.; Lindbergh, G.; Cabrera, S. Synthesis and Characterization of $LiFePO_4$–PANI Hybrid Material as Cathode for Lithium-Ion Batteries. *Materials* **2020**, *13*, 2834. [CrossRef]
50. Niu, Z.; Luan, P.; Shao, Q.; Dong, H.; Li, J.; Chen, J.; Zhao, D.; Cai, L.; Zhou, W.; Chen, X.; et al. A "skeleton/skin" strategy for preparing ultrathin free-standing single-walled carbon nanotube/polyaniline films for high performance supercapacitor electrodes. *Energy Environ. Sci.* **2012**, *5*, 8726–8733. [CrossRef]
51. Li, G.; Li, G.; Ye, S.; Gao, X. A Polyaniline-Coated Sulfur/Carbon Composite with an Enhanced High-Rate Capability as a Cathode Material for Lithium/Sulfur Batteries. *Adv. Energy Mater.* **2012**, *2*, 1238–1245. [CrossRef]
52. Banerjee, J.; Dutta, K.; Kader, M.A.; Nayak, S.K. An overview on the recent developments in polyaniline-based supercapacitors. *Polym. Adv. Technol.* **2019**, *30*, 1902–1921. [CrossRef]
53. Hao, Q.; Wang, H.; Yang, X.; Lu, L.; Wang, X. Morphology-controlled fabrication of sulfonated graphene/polyaniline nanocomposites by liquid/liquid interfacial polymerization and investigation of their electrochemical properties. *Nano Res.* **2011**, *4*, 323–333. [CrossRef]

54. Zhao, Y.; Arowo, M.; Wu, W.; Zou, H.; Chen, J.; Chu, G. Polyaniline/graphene nanocomposites synthesized by in situ high gravity chemical oxidative polymerization for supercapacitor. *J. Ind. Eng. Chem.* **2015**, *25*, 280–287. [CrossRef]
55. Feng, X.; Li, R.; Ma, Y.; Chen, R.; Shi, N.; Fan, Q.; Huang, W. One-Step Electrochemical Synthesis of Graphene/Polyaniline Composite Film and Its Applications. *Adv. Funct. Mater.* **2011**, *21*, 2989–2996. [CrossRef]
56. Gul, H.; Shah, A.A.; Krewer, U.; Bilal, S. Study on Direct Synthesis of Energy Efficient Multifunctional Polyaniline–Graphene Oxide Nanocomposite and Its Application in Aqueous Symmetric Supercapacitor Devices. *Nanomaterials* **2020**, *10*, 118. [CrossRef] [PubMed]
57. Dong, C.; Zhang, X.; Yu, Y.; Huang, L.; Li, J.; Wu, Y.; Liu, Z. An ionic liquid-modified RGO/polyaniline composite for high-performance flexible all-solid-state supercapacitors. *Chem. Commun.* **2020**, *56*, 11993–11996. [CrossRef]
58. Gholami Laelabadi, K.; Moradian, R.; Manouchehri, I. One-Step Fabrication of Flexible, Cost/Time Effective, and High Energy Storage Reduced Graphene Oxide@PANI Supercapacitor. *ACS Appl. Energy Mater.* **2020**, *3*, 5301–5312. [CrossRef]
59. Moyseowicz, A.; Gryglewicz, G. Hydrothermal-assisted synthesis of a porous polyaniline/reduced graphene oxide composite as a high-performance electrode material for supercapacitors. *Compos. Part B Eng.* **2019**, *159*, 4–12. [CrossRef]
60. Snook, G.A.; Kao, P.; Best, A.S. Conducting-polymer-based supercapacitor devices and electrodes. *J. Power Sources* **2011**, *196*, 1–12. [CrossRef]
61. Afzal, A.; Abuilaiwi, F.A.; Habib, A.; Awais, M.; Waje, S.B.; Atieh, M.A. Polypyrrole/carbon nanotube supercapacitors: Technological advances and challenges. *J. Power Sources* **2017**, *352*, 174–186. [CrossRef]
62. Choudhary, R.B.; Ansari, S.; Purty, B. Robust electrochemical performance of polypyrrole (PPy) and polyindole (PIn) based hybrid electrode materials for supercapacitor application: A review. *J. Energy Storage* **2020**, *29*, 101302. [CrossRef]
63. Meng, Q.; Cai, K.; Chen, Y.; Chen, L. Research progress on conducting polymer based supercapacitor electrode materials. *Nano Energy* **2017**, *36*, 268–285. [CrossRef]
64. Sadki, S.; Schottland, P.; Brodie, N.; Sabouraud, G. The mechanisms of pyrrole electropolymerization. *Chem. Soc. Rev.* **2000**, *29*, 283–293.
65. Shi, W.; Han, G.; Chang, Y.; Song, H.; Hou, W.; Chen, Q. Using Stretchable PPy@PVA Composites as a High-Sensitivity Strain Sensor To Monitor Minute Motion. *ACS Appl. Mater. Interfaces* **2020**, *12*, 45373–45382. [CrossRef] [PubMed]
66. Abu Elella, M.H.; Goda, E.S.; Yoon, K.R.; Hong, S.E.; Morsy, M.S.; Sadak, R.A.; Gamal, H. Novel vapor polymerization for integrating flame retardant textile with multifunctional properties. *Compos. Commun.* **2021**, *24*, 100614. [CrossRef]
67. Sultana, I.; Rahman, M.M.; Wang, J.; Wang, C.; Wallace, G.G.; Liu, H. Indigo carmine (IC) doped polypyrrole (PPy) as a free-standing polymer electrode for lithium secondary battery application. *Solid State Ion.* **2012**, *215*, 29–35. [CrossRef]
68. Wen, J.; Ding, Y.; Zhong, J.; Chen, R.; Gao, F.; Qiao, Y.; Fu, C.; Wang, J.; Shen, L.; He, H. Ice-interface assisted large-scale preparation of polypyrrole/graphene oxide films for all-solid-state supercapacitors. *RSC Adv.* **2020**, *10*, 41503–41510. [CrossRef]
69. Feng, H.; Wang, B.; Tan, L.; Chen, N.; Wang, N.; Chen, B. Polypyrrole/hexadecylpyridinium chloride-modified graphite oxide composites: Fabrication, characterization, and application in supercapacitors. *J. Power Sources* **2014**, *246*, 621–628. [CrossRef]
70. Ghanbari, R.; Shabestari, M.E.; Kalali, E.N.; Hu, Y.; Ghorbani, S.R. Electrochemical performance and complex impedance properties of reduced-graphene oxide/polypyrrole nanofiber nanocomposite. *Ionics* **2021**, *27*, 1279–1290. [CrossRef]
71. Gómez Costa, M.B.; Juárez, J.M.; Martínez, M.L.; Cussa, J.; Anunziata, O.A. Synthesis and characterization of a novel composite: Polyindole included in nanostructured Al-MCM-41 material. *Microporous Mesoporous Mater.* **2012**, *153*, 191–197. [CrossRef]
72. Gupta, B.; Chauhan, D.S.; Prakash, R. Controlled morphology of conducting polymers: Formation of nanorods and microspheres of polyindole. *Mater. Chem. Phys.* **2010**, *120*, 625–630. [CrossRef]
73. Tebyetekerwa, M.; Wang, X.; Marriam, I.; Dan, P.; Yang, S.; Zhu, M. Green approach to fabricate Polyindole composite nanofibers for energy and sensor applications. *Mater. Lett.* **2017**, *209*, 400–403. [CrossRef]
74. Dhanalakshmi, K.; Saraswathi, R. Electrochemical preparation and characterization of conducting copolymers: Poly(pyrrole-co-indole). *J. Mater. Sci.* **2001**, *36*, 4107–4115. [CrossRef]
75. Marriam, I.; Wang, Y.; Tebyetekerwa, M. Polyindole batteries and supercapacitors. *Energy Storage Mater.* **2020**, *33*, 336–359. [CrossRef]
76. Mudila, H.; Rana, S.; Zaidi, M.G.H.; Alam, S. Polyindole/Graphene Oxide Nanocomposites: The Novel Material for Electrochemical Energy Storage. *Fuller. Nanotub. Carbon Nanostruct.* **2015**, *23*, 20–26. [CrossRef]
77. Zhou, Q.; Zhu, D.; Ma, X.; Xu, J.; Zhou, W.; Zhao, F. High-performance capacitive behavior of layered reduced graphene oxide and polyindole nanocomposite materials. *RSC Adv.* **2016**, *6*, 29840–29847. [CrossRef]
78. Gao, Y. Graphene and Polymer Composites for Supercapacitor Applications: A Review. *Nanoscale Res. Lett.* **2017**, *12*, 387. [CrossRef]
79. Zhou, C.; Zhang, Y.; Li, Y.; Liu, J. Construction of High-Capacitance 3D CoO@Polypyrrole Nanowire Array Electrode for Aqueous Asymmetric Supercapacitor. *Nano Lett.* **2013**, *13*, 2078–2085. [CrossRef]
80. Liu, M.; Miao, Y.E.; Zhang, C.; Tjiu, W.W.; Yang, Z.; Peng, H.; Liu, T. Hierarchical composites of polyaniline-graphene nanoribbons-carbon nanotubes as electrode materials in all-solid-state supercapacitors. *Nanoscale* **2013**, *5*, 7312–7320. [CrossRef]
81. Murugan, A.V.; Muraliganth, T.; Manthiram, A. Rapid, Facile Microwave-Solvothermal Synthesis of Graphene Nanosheets and Their Polyaniline Nanocomposites for Energy Strorage. *Chem. Mater.* **2009**, *21*, 5004–5006. [CrossRef]

82. Hassan, M.; Reddy, K.R.; Haque, E.; Faisal, S.N.; Ghasemi, S.; Minett, A.I.; Gomes, V.G. Hierarchical assembly of graphene/polyaniline nanostructures to synthesize free-standing supercapacitor electrode. *Compos. Sci. Technol.* **2014**, *98*, 1–8. [CrossRef]
83. Huang, Y.; Tao, J.; Meng, W.; Zhu, M.; Huang, Y.; Fu, Y.; Gao, Y.; Zhi, C. Super-high rate stretchable polypyrrole-based supercapacitors with excellent cycling stability. *Nano Energy* **2015**, *11*, 518–525. [CrossRef]
84. Biswas, S.; Drzal, L.T. Multilayered Nanoarchitecture of Graphene Nanosheets and Polypyrrole Nanowires for High Performance Supercapacitor Electrodes. *Chem. Mater.* **2010**, *22*, 5667–5671. [CrossRef]
85. Liu, Y.; Zhang, Y.; Ma, G.; Wang, Z.; Liu, K.; Liu, H. Ethylene glycol reduced graphene oxide/polypyrrole composite for supercapacitor. *Electrochim. Acta* **2013**, *88*, 519–525. [CrossRef]
86. Majumder, M.; Choudhary, R.B.; Koiry, S.P.; Thakur, A.K.; Kumar, U. Gravimetric and volumetric capacitive performance of polyindole/carbon black/MoS_2 hybrid electrode material for supercapacitor applications. *Electrochim. Acta* **2017**, *248*, 98–111. [CrossRef]
87. Azizi, E.; Arjomandi, J.; Salimi, A.; Lee, J.Y. Fabrication of an asymmetric supercapacitor based on reduced graphene oxide/polyindole/gamma—Al_2O_3 ternary nanocomposite with high-performance capacitive behavior. *Polymer* **2020**, *195*, 122429. [CrossRef]
88. Wang, H.; Liu, R.; Liu, X.; Wu, L.; Li, Y.; Zhang, X. Improved Electrochemical Performances of Graphene Hybrids Embedded with Silica as the Functional Connection Layer for Supercapacitors. *J. Energy Storage* **2021**, *36*, 102315. [CrossRef]
89. Xu, Z.; Zhang, Z.; Yin, H.; Hou, S.; Lin, H.; Zhou, J.; Zhuo, S. Investigation on the role of different conductive polymers in supercapacitors based on a zinc sulfide/reduced graphene oxide/conductive polymer ternary composite electrode. *RSC Adv.* **2020**, *10*, 3122–3129. [CrossRef]
90. Ramesh, S.; Yadav, H.; Bathula, C.; Shinde, S.; Sivasamy, A.; Kim, H.; Kim, H.S.; Kim, J. Cubic nanostructure of Co_3O_4@nitrogen doped graphene oxide/polyindole composite efficient electrodes for high performance energy storage applications. *J. Mater. Res. Technol.* **2020**, *9*, 11464–11475. [CrossRef]
91. Ehsani, A.; Heidari, A.A.; Shiri, H.M. Electrochemical pseudocapacitors based on ternary nanocomposite of conductive polymer/graphene/metal oxide: An introduction and review to it in recent studies. *Chem. Rec.* **2019**, *19*, 908–926. [CrossRef] [PubMed]
92. Dong, L.; Chen, Z.; Yang, D.; Lu, H. Hierarchically structured graphene-based supercapacitor electrodes. *RSC Adv.* **2013**, *3*, 21183–21191. [CrossRef]
93. Dywili, N.R.; Ntziouni, A.; Ikpo, C.; Ndipingwi, M.; Hlongwa, N.W.; Yonkeu, A.; Masikini, M.; Kordatos, K.; Iwuoha, E.I. Graphene Oxide Decorated Nanometal-Poly(Anilino-Dodecylbenzene Sulfonic Acid) for Application in High Performance Supercapacitors. *Micromachines* **2019**, *10*, 115. [CrossRef]
94. Golkhatmi, S.Z.; Sedghi, A.; Miankushki, H.N.; Khalaj, M. Structural properties and supercapacitive performance evaluation of the nickel oxide/graphene/polypyrrole hybrid ternary nanocomposite in aqueous and organic electrolytes. *Energy* **2021**, *214*, 118950. [CrossRef]
95. Li, S.; Zhang, L.; Zhang, L.; Zhang, J.; Zhou, H.; Chen, X.; Tang, T. The in situ construction of three-dimensional core-shell-structured TiO_2@PPy/rGO nanocomposites for improved supercapacitor electrode performance. *New J. Chem.* **2021**, *45*, 1092–1099. [CrossRef]
96. Golikand, A.N.; Bagherzadeh, M.; Shirazi, Z. Evaluation of the Polyaniline Based Nanocomposite Modified with Graphene Nanosheet, Carbon Nanotube, and Pt Nanoparticle as a Material for Supercapacitor. *Electrochim. Acta* **2017**, *247*, 116–124. [CrossRef]
97. Gottam, R.; Srinivasan, P. Composite electrode material of MoO_3-MC-SiO_2-PANI: Aqueous supercapacitor cell with high energy density, 1 V and 250,000 CD cycles. *Polym. Adv. Technol.* **2021**, *32*, 2465–2475. [CrossRef]
98. Wang, X.; Wu, D.; Song, X.; Du, W.; Zhao, X.; Zhang, D. Review on Carbon/Polyaniline Hybrids: Design and Synthesis for Supercapacitor. *Molecules* **2019**, *24*, 2263. [CrossRef] [PubMed]